Molecular Biology of the Cell
Vol. 15, 5172–5286, November 2004

A NIMA-related Kinase, Fa2p, Localizes to a Novel Site in the Proximal Cilia of *Chlamydomonas* and Mouse Kidney Cells

Moe R. Mahjoub, M. Qasim Rasi, and Lynne M. Quarmby*

Department of Molecular Biology and Biochemistry, Simon Fraser University, Burnaby, British Columbia, Canada V5A 1S6

Submitted July 8, 2004; Revised August 26, 2004; Accepted August 31, 2004
Monitoring Editor: Trisha Davis

Polycystic kidney disease and related syndromes involve dysregulation of cell proliferation in conjunction with ciliary defects. The relationship between cilia and cell cycle is enigmatic, but it may involve regulation by the NIMA-family of kinases (Neks). We previously showed that the Nek Fa2p is important for ciliary function and cell cycle in *Chlamydomonas*. We now show that Fa2p localizes to an important regulatory site at the proximal end of cilia in both *Chlamydomonas* and a mouse kidney cell line. Fa2p also is associated with the proximal end of centrioles. Its localization is dynamic during the cell cycle, following a similar pattern in both cell types. The cell cycle function of Fa2p is kinase independent, whereas its ciliary function is kinase dependent. Mice with mutations in Nek1 or Nek8 have cystic kidneys; therefore, our discovery that a member of this phylogenetic group of Nek proteins is localized to the same sites in *Chlamydomonas* and kidney epithelial cells suggests that Neks play conserved roles in the coordination of cilia and cell cycle progression.

INTRODUCTION

The Nek family of kinases is defined by sequence similarity to NIMA, the *Aspergillus* kinase that is essential for entry into mitosis (reviewed by Morris and Enos, 1992; O'Connell *et al*., 2003). Fungi and higher plants encode only one or a few members of this family (Kambouris *et al*., 1993; Pu *et al*., 1995; Krien *et al*., 1998; Wang *et al*., 2003), but in organisms with centrioles and cilia, such as humans and *Chlamydomonas*, the family is expanded to 10 or more members (O'Connell *et al*., 2003; Bradley *et al*., 2004; Bradley and Quarmby, unpublished data), some of which affect ciliary length (Wloga, Rogowski, and Gaertig, ASCB meeting, 2003, Abstract 2439). We recently reported that the *Chlamydomonas* Nek Fa2p participates in ciliary function and cell cycle progression (Mahjoub *et al*., 2002).

An emerging pattern suggests that a variety of human syndromes are related to defects in the assembly, maintenance, or function of cilia (Ong and Wheatley, 2003; Pazour and Witman, 2003; Li *et al*., 2004; Sun *et al*., 2004). Ciliopathies, including polycystic kidney disease, Bardet-Beidl syndrome, and nephronophthisis include kidney cyst formation as an important component of a pleiotropic syndrome (Mykytyn and Sheffield, 2004; Wilson, 2004). This important consequence of these diseases arises, in part, from dysregulation of cell proliferation in conjunction with ciliary dysfunction. Of particular relevance to the current study are reports that mutations in vertebrate Nek1 and Nek8 cause cystic kidneys in mice and zebrafish (Upadhya *et al*., 2000; Liu *et al*., 2002).

Article published online ahead of print. Mol. Biol. Cell 10.1091/mbc.E04–07–0571. Article and publication date are available at www.molbiolcell.org/cgi/doi/10.1091/mbc.E04–07–0571.

* Corresponding author. E-mail address: quarmby@sfu.ca.

The relationship between cilia and cell cycle progression is poorly understood. In many cells, entry into the cell cycle is preceded by ciliary disassembly, and exit from mitosis is accompanied by ciliary assembly, a relationship that may reflect the use of the basal bodies/centrioles as mitotic spindle poles (Tucker and Pardee, 1979; Ehler *et al*., 1995; Wheatley *et al*., 1996). Consistent with this idea, signaling pathways important for growth or differentiation have been reported to localize to cilia (Huangfu *et al*., 2003; Pazour and Witman, 2003; Schneider, Hoffmann, Satir, Christensen, unpublished data) and some *Chlamydomonas* mutants defective in ciliary assembly have cell cycle progression phenotypes (Mahjoub *et al*., 2002; Parker and Quarmby, unpublished data). In addition, members of protein families known for their mitotic functions have been found to play roles in ciliary assembly, including EB1 (Pedersen *et al*., 2003); a distant paralog of aurora kinase, CALK (Pan *et al*., 2004); and a mitogen-activated protein kinase (Berman *et al*., 2003). The simplest hypothesis is that cells can be maintained in a differentiated state by signals received from their cilia and that loss of cilia or ciliary signaling can be a trigger for reentry into the cell cycle. This is likely to be a reciprocal relationship in which signals from the cell body stimulate ciliary loss in anticipation of cell division and ciliary regrowth upon exit from mitosis. The Nek proteins may play roles in this reciprocal signaling.

Fa2p was originally identified from a screen for deflagellation-defective mutants in *Chlamydomonas reinhardtii* and shown to be defective in calcium-induced severing of the axonemal microtubules (Finst *et al*., 1998). We noticed that *fa2* cells are larger than wild-type and went on to show that this is due to a delay at the G_2/M transition (Mahjoub *et al*., 2002). The preponderance of Nek family members in organisms with cilia, and the intriguing combination of ciliary and cell cycle phenotypes of *fa2* mutants, lead us to pursue this protein in our efforts to dissect the enigmatic relationship between cilia and the cell cycle.

Here, we report that Fa2p localizes to a specific site at the proximal end of the cilia, in both *Chlamydomonas* and cultured kidney epithelial cells. When cells enter the cell cycle, Fa2p accumulates at the base of the basal bodies/centrioles. It remains associated with the spindle poles throughout the cell cycle and moves to the cilia when they begin to regenerate after deciliation or exit from the cell cycle. Importantly, Fa2p kinase activity is required for deflagellation, but not for localization and efficient cell cycle progression.

MATERIALS AND METHODS

Cell Strains and Culture

Chlamydomonas strains B214 and G1 (obtained from G. Pazour, University of Massachusetts, Amherst, MA) and strains cc620 and cc621 (obtained from the *Chlamydomonas* Genetics Center, Durham, NC) were used as the wild-type strains. Mutant strains *fa2-1*, *fa2-2*, *fa2-3*, and *fa2-4* were isolated in our laboratory as described previously (Finst *et al*., 1998). Cells were maintained in liquid TAP medium or on plates containing 1.5% agar (Harris, 1989) at 22°C with constant illumination. All *ble* transformants were grown on 1.5% TAP plates supplemented with Zeocin (30 μg/ml; Invitrogen, Carlsbad, CA).

All chemicals were purchased from Sigma-Aldrich (St. Louis, MO) unless otherwise indicated.

Epitope Tagging and Chlamydomonas *Transformations*

The 4.6-kb wild-type genomic construct pFA2 (*Sac*I-*Sal*I) (Mahjoub *et al*., 2002) was engineered to contain three copies of the hemagglutinin (HA) epitope in the carboxy terminus of the predicted product. The FA2 (*Sac*I-*Sal*I) plasmid was linearized at a unique *Nru*I site at base position 3108 in the second to last exon. Next, the p3 × HA (a plasmid encoding 3 repeats of the 9-amino acid hemagglutinin epitope; Finst *et al*., 2000) was digested with *Sma*I and *Nae*I to excise the 3 × HA cassette. The *Sma*I-*Nae*I fragment was blunt-end ligated into the *Nru*I-linearized FA2 construct to produce plasmid pFA2HA (3108), which encodes a Fa2p-HA chimera with the HA tag following directly after amino acid 536. To introduce the selectable marker *ble* into this construct, plasmid pSP124S (kindly provided by Saul Purton, University College London, United Kingdom; England; Lumbreras *et al*., 1998) was digested with *Hind*III to release the gene cassette. This cassette was subsequently ligated into the p3 × HAFA2(3108) after digestion at a unique *Hind*III site upstream of the 5′UTR, to produce the final plasmid pble-FA2HA (3108).

Nuclear transformation was performed as described previously (Finst *et al*., 1998). Transformants were selected on 1.5% TAP medium plates supplemented with Zeocin and assayed for deflagellation as described previously (Finst *et al*., 1998).

Antibodies and Immunoblot Analysis

Based on the predicted Fa2p amino acid sequence, peptides 364–380 (QIPYLPHQRPGSGRSPG) and 562–575 (YQAPQYGRRRNPE) were synthesized, conjugated to keyhole limpet hemocyanin and used as antigens to raise rabbit polyclonal antibodies (Sigma Genosys, The Woodlands, TX). Polyclonal antiserum from one positively reactive rabbit (10495, immunized by peptide 562-575) was affinity purified using a peptide column per manufacturer's instructions (UltraLink biosupport medium; Pierce Chemical, Rockford, IL) to produce anti-Fa2p-10495, used in these experiments as anti-Fa2p.

For immunoblot analysis, whole cell lysate from wild type, a series of mutant cells carrying various *fa2* alleles, *fa2*-1; *FA2* (*fa2*-1 cells transformed with the wild-type *FA2* genomic clone), and *fa2*-1; *FA2*-HA strains (*fa2*-1 cells transformed with the FA2-HA construct) were used. Protein concentration was determined using the Advanced Protein Assay (Cytoskeleton, Denver, CO). Whole cell extract (30 μg) was separated by SDS-PAGE (10%) and electroblotted to supported nitrocellulose (Bio-Rad, Hercules, CA). To confirm efficient transfer of protein samples, membranes were stained with Ponceau S (Allied Chemicals, Morristown, NJ) and then washed with 0.05% Tween 20 in Tris-buffered saline/Tween (TBST). The membrane was blocked in 5% skim milk in TBST for 1 h at room temperature, and then incubated overnight at 4°C with affinity-purified anti-Fa2p-10495 (1:250). The membrane was washed with TBST and incubated with horseradish peroxidase-linked donkey anti-rabbit IgG (1:10,000; Amersham Biosciences, Baie d'Urfé, Québec, Canada) at room temperature with rocking for 1 h. For detection of Fa2p-HA, the membrane was incubated overnight with rat monoclonal anti-HA (1:1000; clone 3F10; Roche Diagnostics, Berkeley, CA), washed with TBST, and then incubated with horseradish peroxidase-linked goat anti-rat IgG (1:2500; Amersham Biosciences). For loading control, blots were stripped using the ReBlot Plus kit (Chemicon International; Temecula, CA), and then probed with mouse monoclonal anti-α-tubulin (1:10,000; clone B-5-1-2; Sigma-Aldrich). After washes with TBST, blots were incubated with horseradish peroxidase-linked horse anti-mouse IgG (1:10,000; Vector Laboratories, Burlingame, CA). Immunoreactive proteins were visualized using the ECL chemiluminescent detection system (Amersham Biosciences).

Subcellular Fractionation

Deflagellation was induced by dibucaine, and cell bodies, flagella, axonemes, and membrane plus matrix fractions were isolated as described previously (Witman, 1986). We substituted 1% IGEPAL CA 630 (Sigma-Aldrich) for 0.5% NP-40. Cell equivalents of each fraction were used for immunoblot analysis.

Indirect Immunofluorescence Imaging of Chlamydomonas Cells

For indirect immunofluorescence, *fa2* mutants and *fa2*-1; *FA2*-HA strains were harvested from suspension by centrifugation and treated with gametic lytic enzyme to remove their cell walls (Saito and Matsuda, 1991). The cells were pelleted by centrifugation and resuspended in MT buffer (30 mM Tris-acetate, pH 7.3, 5 mM $MgSO_4$, 5 mM EDTA, 25 mM KCl, 1 mM dithiothreitol), and then affixed to coverslips coated with 0.1% polyethylenimine. Cells were fixed in 100% ice-cold methanol at −20°C for 20 min, rehydrated by three 5-min washes in phosphate-buffered saline (PBS), and blocked with 3% bovine serum albumin in PBS for 1 h. The coverslips with fixed cells were incubated overnight at 4°C with rat monoclonal anti-HA (diluted 50-fold), together with the mouse monoclonal anti-α-tubulin (diluted 500-fold) and a mouse monoclonal anti-centrin (clone 20H5, diluted 400-fold; generously provided by J. Salisbury, Mayo Clinic, Rochester, MN). The next day, coverslips were rinsed three times in PBS and then incubated for 1 h with the appropriate secondary antibody, depending on the experiment: Texas Red- or -Alexa Fluor 488-conjugated goat anti-rat IgG (for Fa2p-HA), Alexa Fluor 350- or 488-conjugated goat anti-mouse IgG (for centrin), and Alexa Fluor 488, 568, or CY-5–conjugated goat anti-mouse IgG (for α-tubulin). All secondary antibodies were purchased from Molecular Probes (Eugene, OR) and diluted 200-fold in PBS before use. The cells were rinsed in PBS and mounted in an antifade medium containing 0.1 mg/ml Mowiol (Calbiochem, San Diego, CA), 50% glycerol, and 100 mM Tris, pH 8.5.

To visualize cells immediately after deflagellation, live cultures of a *fa2*-1; *FA2*-HA strain were affixed to coverslips coated with 0.1% polyethylenimine for 1 min. Deflagellation was induced by addition of a drop of 25 mM dibucaine, and samples were immediately fixed with ice-cold methanol. To study localization of Fa2p-HA during flagellar regeneration, cells were deflagellated by pH shock as described previously (Finst *et al*., 1998). Cells were pelleted, resuspended in TAP medium and allowed to regenerate their flagella. Samples were taken at 5, 30, 60, and 90 min postdeflagellation. Cells were fixed, processed, and stained as described above.

A series of digital optical sections of the fixed samples were obtained using an Olympus IX70 epifluorescence inverted microscope in a DeltaVision imaging station (Applied Precision, Issaquah, WA). The system is fitted with a computer-controlled stage with Nanomotion micropositioning technology with a stepping motor (0.2-μm step size), 100× (1.35 numerical aperture) Olympus objective and fluorescein, rhodamine, 4,6-diamidino-2-phenylindole (DAPI), and CY-5 filter set. Stacks of digital images were acquired with a cooled charge-coupled device camera (Roper Scientific, Tucson, AZ). Out-of-focus fluorescence and restoration of optical Z-sections was achieved by deconvolution by using the constrained iterative algorithm and point spread functions supplied with the DeltaVision system. Three-dimensional reconstructions were produced by stacking a set of deconvolved sections and projecting them around the *x*- or *y*-axis.

Differential interference contrast optics were used for cell size measurements, as described previously (Mahjoub *et al*., 2002). Cells were fixed with 2% glutaraldehyde in culture medium and measured using software provided with the Delta Vision system (Applied Precision).

Cell Synchrony and Mating

Synchronization of cells was carried out as described by Umen and Goodenough (2001) with modification. Cultures were grown in M-medium (Harris, 1989) at 25°C with shaking. Flasks were bubbled with 5% CO_2 and grown asynchronously to a density of 5×10^6 cells/ml in the light, and then placed in the dark at 1×10^6 cells/ml for 24 h. Cultures were then moved back to the light, and aliquots were sampled over the next 24 h. Cells were fixed, processed, and stained as described above.

For zygotic resorption experiments, vegetative wild-type and *fa2*-1; *FA2*-HA strains were pelleted and resuspended in medium lacking nitrogen (M-N is M medium, Harris, 1989, excluding NH_4NO_3) for 16 h to induce gametogenesis. The resulting gametes were mixed together and allowed to form quadriflagellate cells (QFCs). Samples were taken at 30-min intervals over the next 4 h. Cells were fixed, processed, and stained as described above.

For mitotic index experiments, we examined 300 fixed cells (from each sample) microscopically for cleavage furrows to determine the fraction of cells that had entered M phase. In *Chlamydomonas*, incipient cleavage furrows form at preprophase and are visible throughout mitosis and cytokinesis (Kirk, 1998).

Construction of Kinase-dead Fa2p

The QuikChange site-directed mutagenesis kit (Stratagene, La Jolla, CA) was used to introduce an A-to-G change at base position 137 (from the start codon). The resulting translated product substitutes the invariant lysine (aa 46

in Fa2p) of the ATP-binding loop to arginine. The plasmid pFA2 (*Sac*I-*Sal*I) was used as template, and site-directed mutagenesis was performed following manufacturer's instructions, to produce pFA2-K46R. To introduce this change in the FA2 construct containing the HA-tag and *ble* marker, a *Bam*HI-*Pml*I cassette (containing the A-to-G change) was excised and substituted into pble-FA2HA (3108) digested with *Bam*HI-*Pml*I, to produce the final vector pble-FA2HA-K46R. Integrity of the final construct was confirmed by DNA sequencing (DNA sequencing laboratory, University of British Columbia). The construct was transformed into *fa2* mutants, and transformants were analyzed as described above.

Fa2p Expression in Mammalian Cells

To express green fluorescent protein (GFP)-tagged Fa2p in mouse kidney collecting duct epithelial cells (murine inner medullary collecting duct cells; mIMCD-3), *FA2* cDNA was isolated using methods described by Finst *et al*. (2000). Primers were used to introduce an *Eco*RI (5′) and *Sal*I (3′) sites in the *FA2* cDNA, which was subsequently cloned into the pEGFP-C2 vector (BD Biosciences Clontech, Palo Alto, CA) digested with *Eco*RI-*Sal*I, to give vector pEGFP-FA2. The resulting product is an EGFP-Fa2p chimeric protein.

IMCD-3 cells were maintained in 1:1 mixture of DMEM (Invitrogen) and Ham's F-12 medium (Invitrogen), supplemented with 10% fetal bovine serum (FBS), at 37°C in the presence of 5% CO_2. Cells were cultured to 70–80% confluence and transfected with either pEGFP or pEGFP-FA2 by using the Polyfect transfection reagent per manufacturer's instruction (QIAGEN, Valencia, CA). Cells were collected 24 h after transfection, resuspended in 1× SDS sample buffer, and analyzed by immunoblot with anti-GFP (1:2000; Roche Diagnostics) as described above. Alternatively, cells were grown on coverslips, transfected as described above, and then fixed in −20°C methanol for 10 min, rehydrated in PBS, and blocked with 5.5% FBS in PBS. Samples were incubated 1 h with mouse monoclonal anti-acetylated tubulin (Sigma, clone 6–11B-1, diluted 10,000-fold) and mouse monoclonal anti-gamma tubulin (clone GTU-88, diluted 1000-fold; Sigma-Aldrich). After washing with PBS, cells were incubated for 1 h with Alexa Fluor 568-conjugated rabbit anti-mouse IgG (diluted 200-fold), and then rinsed in PBS. Nuclei were stained by incubating with DAPI for 10 min. Coverslips were mounted in Prolong antifade reagent (Molecular Probes), and immunofluorescence microscopy was performed as described above.

RESULTS

Epitope Tagging, Transformation Rescue, and Antibody Characterization

To determine the spatial and temporal localization of Fa2p, we undertook two approaches. First, we inserted an HA epitope tag near the carboxy terminus of the predicted Fa2p product (Figure 1A). The construct also carried the antibiotic resistance gene *ble*, allowing selection of transformants on Zeocin plates. *fa2-1* mutants were transformed with this construct and assayed for deflagellation phenotype by pH shock and for Fa2p-HA expression by immunoblot. Of the transformants, ~30% (n = 65) expressed the expected 73-kDa fusion protein (Figure 1B). All of the colonies expressing the fusion protein showed rescue of the deflagellation defect (Figure 1B).

We also raised antibodies against Fa2p peptides. Based on the Fa2p amino acid sequence, peptides 364–380 (in the middle region) and 562–575 (near the extreme C terminus) were used as antigens. Polyclonal antibodies against Fa2p were affinity purified from one positively reactive rabbit injected with peptide 562–575. The affinity purified anti-Fa2p recognizes a single protein of expected size on immunoblots of wild-type cells (Figure 1C). As expected, this band is not detected in any of four *fa2* mutant strains (Mahjoub *et al*., 2002), but is present in *fa2-1* cells that were transformed with the *FA2* gene. Additionally, the antibody recognizes the HA-tagged Fa2 protein (Figure 1C).

Subcellular Localization of Fa2p

Given that *fa2* mutants have defects in deflagellation and in cell cycle progression (Mahjoub *et al*., 2002), it was of interest to determine whether Fa2p was associated with the flagella or the cell body. Wild-type cells were deflagellated by treatment with 5 mM dibucaine (Witman, 1986) and cell-equivalent amounts of whole cell, cell bodies, and flagella were analyzed by immunoblot. Fa2p is detected in the flagellar fraction but not cell bodies of wild-type cells (Figure 2A, left). The same result was obtained in cell fractions of the *fa2*-1; *FA2*-HA strains (Figure 2A, right). Flagella were further fractionated by detergent extraction to yield a membrane plus matrix fraction and an axonemal fraction. Western analysis showed that Fa2p is an axonemal protein (Figure 2B).

Fa2p Localizes to a Unique Site at the Proximal End of Flagella

We next performed indirect immunofluorescence to refine the localization of Fa2p in the axoneme. Repeated attempts at immunofluorescence with the anti-Fa2p antibodies were unsuccessful, so we used the *fa2*-1; *FA2*-HA strains for the following localization experiments. We are confident that the Fa2p-HA localization with anti-HA antibody accurately reflects the localization of endogenous Fa2p because 1) Fa2p-HA is expressed at levels below or comparable with endogenous Fa2p (Figure 1C) (2) Fa2p-HA rescued the deflagellation defect of *fa2* cells (Figure 1B), and 3) the subcellular fractionation of Fa2p-HA was indistinguishable from Fa2p (Figure 2).

Indirect immunofluorescence staining of *fa2*-1; *FA2*-HA cells with anti-HA reveals two distinct sites of localization of Fa2p-HA. All of the >1000 cells examined showed staining near the base of each flagellum (Figure 3A, top). In addition, some of the cells reveal a signal in the basal body region (Figure 3). Centrin is known to localize with the distal striated fibers that connect the two basal bodies, as well as to form the nucleus-basal body connectors (Salisbury *et al*., 1988; Sanders and Salisbury, 1989). Based on comparison with the centrin signal, the distinct Fa2p-HA flagellar signals occur above the distal striated fiber, near the transition zone region at the proximal end of the flagella (Figure 3). We refer to this protein as axonemal-Fa2p (ax-Fa2p). The basal body-associated signal is clearly below the distal striated fibers, in the region where the proximal ends of the two basal bodies are in juxtaposition (Figure 3). We refer to this subset of the total Fa2p-HA as basal body associated-Fa2p (bb-Fa2p). In a population of asynchronously growing cells, bb-Fa2p comprises a small fraction of total Fa2p, as indicated by the immunoblots (Figure 2).

Deflagellation is a consequence of calcium-induced severing of axonemal microtubules at the distal end of the transition zone, near the base of the flagella (reviewed in Quarmby, 2004). Our biochemical fractionation (Figure 2) indicated that the ax-Fa2p was located on the axonemal side of this site. To confirm this, live *fa2*-1; *FA2*-HA cells were allowed to adhere briefly to coverslips, deflagellated with dibucaine (<2 s), and fixed immediately. Due to the briefness of the deflagellation treatment, not all cells shed both flagella. In cells that did not shed their flagella, Fa2p-HA was observed at the base of the flagella as described above (Figure 4, left column). In cases where a cell had shed one flagellum, the Fa2p-HA signal remained with the corresponding severed flagellum and was localized to the proximal tip (Figure 4, middle column). Note that no Fa2p-HA signal from the severed flagellum was retained by the cell body, indicating that ax-Fa2p is distal to the transition zone. Similarly, when both flagella were shed, Fa2p-HA was detected at the proximal ends of each (Figure 4, right column). In the ~800 cells that were examined, every shed flagellum had a signal at the proximal end, and no ax-Fa2p-HA signal was retained by the cell body. The localization of axonemal Fa2p exclusively to the proximal end of the axoneme, and

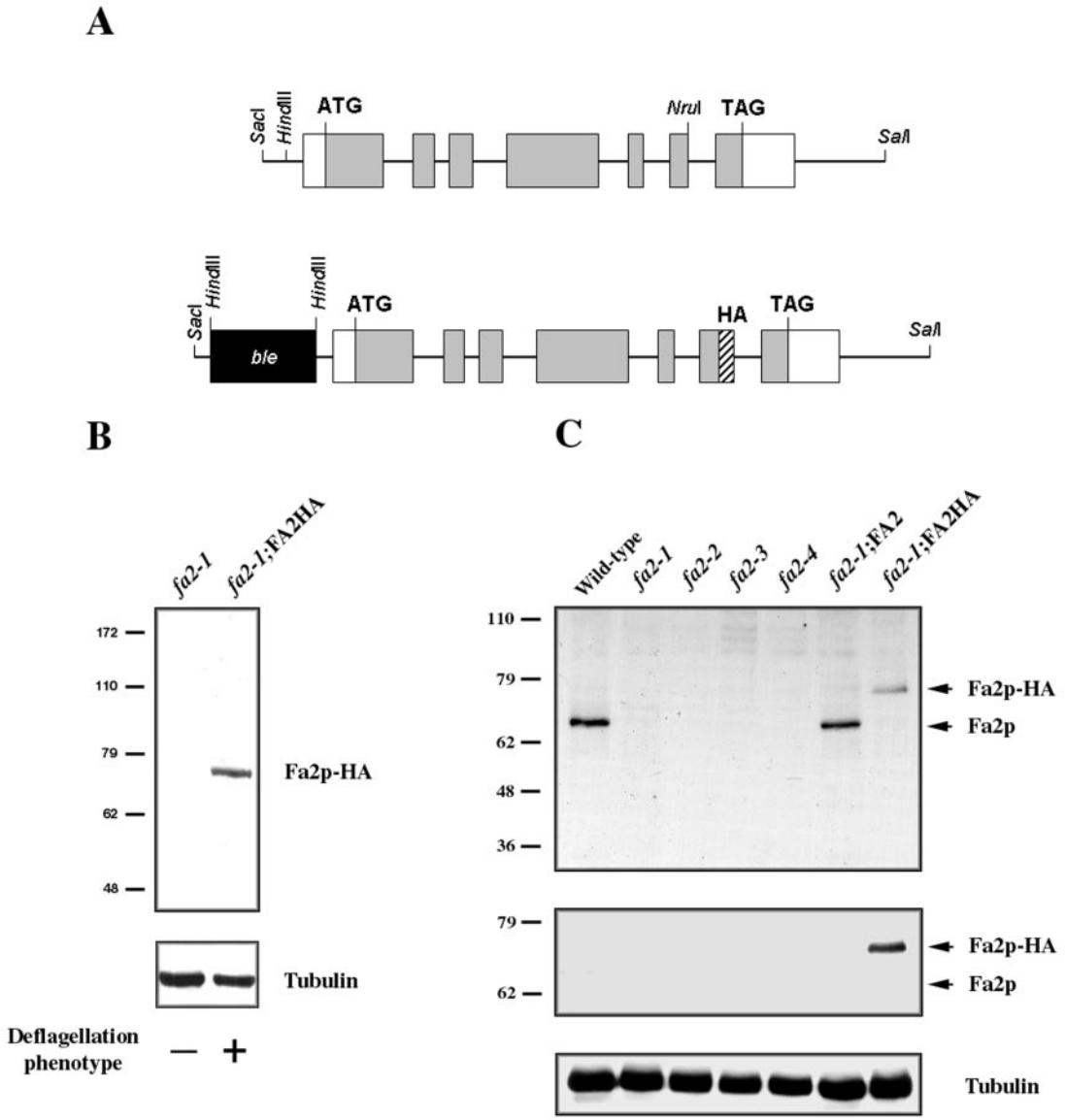

Figure 1. Immunoblot analysis of HA-tagged and endogenous Fa2p. (A) Schematic representation of the genomic *FA2* construct, containing an HA-epitope tag at the C terminus of Fa2p and the *ble* marker gene. Exons are shown in gray and the UTRs in white. (B) Immunoblot of whole cell lysate from *fa2-1* mutants and *fa2-1* cells rescued for deflagellation with the HA-tagged construct. Protein (30 μg) was loaded in each lane, and the blot was probed with anti-HA antibody. The membrane was stripped and reprobed with anti-α-tubulin antibody for loading control. Molecular mass standards (in kilodaltons) are indicated on the left. (C) Characterization of affinity purified anti-Fa2p antibody against whole cell lysate from wild-type, *fa2-1*, *fa2-2*, *fa2-3*, *fa2-4*, *fa2-1* rescued with the *FA2* gene (*fa2*-1; *FA2*), and *fa2-1* rescued with the HA-tagged FA2 construct (*fa2*-1; FA2-HA). Protein (30 μg) was loaded in each lane, and the blot was probed with anti-Fa2p, then stripped, and reprobed with anti-HA. The membrane was stripped again and reprobed with anti-α-tubulin antibody for loading control.

distal to the transition zone microtubule severing region, defines a novel region of the axoneme. Although other axonemal proteins have been found in this region, for example, a minor fraction of epsilon-tubulin (Dutcher *et al*., 2002), Fa2p is the only protein identified so far whose axonemal localization is specific to a site entirely distal to the transition region.

Distribution of Fa2p between the Proximal Axoneme and the Basal Body Correlates with Flagellar Resorption and Regeneration

Chlamydomonas cells are flagellated during interphase; they resorb their flagella before entering mitosis, and grow new flagella at the onset of G_1 (Johnson and Porter, 1968; Cavalier-Smith, 1974). We hypothesized that the subset of cells with bb-Fa2p-HA were cells either entering or exiting mitosis. It is well established that axonemal components are transported into and out of the axoneme by IFT particles and motors and that basal bodies are the docking site for IFT particles and cargo (reviewed by Rosenbaum and Witman, 2002). Consequently, cells with a strong bb-Fa2p signal might be in the process of resorbing or regenerating their flagella. To test this idea, we synchronized the growth of *fa2*-1; *FA2*-HA cells as described previously (Mahjoub *et al*., 2002) and harvested cells when they were resorbing their flagella before mitosis. As predicted, we observed an in-

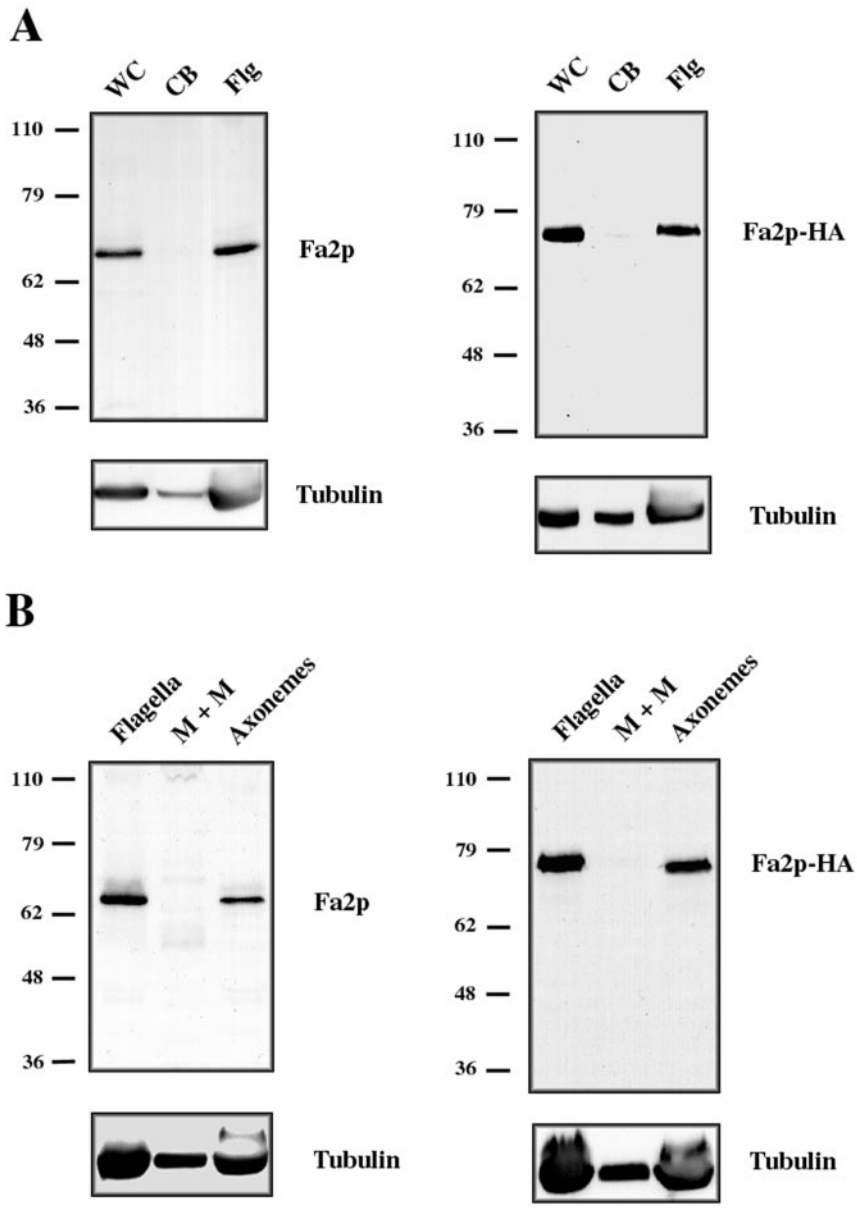

Figure 2. Fa2p is an axonemal protein. (A) Immunoblot of cellular fractions from wild type (left) or *fa2*-1; *FA2*-HA (right) strains shows that Fa2p is found in the flagella. Cells were deflagellated with dibucaine, and equivalent numbers of whole cells (WC), cell bodies (CB), and flagella (Flg) were loaded in each lane. Blots were probed with either anti-Fa2p (left) or anti-HA (right) antibodies. (B) To refine the localization of Fa2p, flagellar membranes were extracted with detergent, and flagellar-equivalent amounts of flagella, membrane plus matrix (M+M), and axonemes were loaded in each lane. Blots were probed with either anti-Fa2p (left) or anti-HA (right) antibodies. All blots were stripped and reprobed with anti-α-tubulin antibody.

crease in the bb-Fa2p signal in cells that were resorbing their flagella (Figure 5A).

We also examined zygotic resorption of flagella. Biflagellate gametes of opposite mating types (+ and −) will fuse and form a temporary QFC or zygote, which will eventually undergo meiosis, producing four haploid cells. Flagellar resorption begins 2–4 h after QFC formation and occurs simultaneously in many cells (Cavalier-Smith, 1974). We mated *fa2*-1; *FA2*-HA and wild-type gametes and allowed 30 min for QFC formation. The wild-type strain does not express an HA epitope and thus acts as an internal control. Within a few minutes of QFC formation, ax-Fa2p signals are observed on only two flagella, presumably the ones derived from the Fa2p-HA expressing gamete (Figure 5B, 8.4 μm). As the flagella shorten, there is an increase in bb-Fa2p levels, similar to what was observed during premitotic flagellar resorption (Figure 5A). Interestingly, the basal bodies from the wild-type cell also begin to show a Fa2p-HA signal as the flagella shorten (Figure 5B, 1.5 and 0.5 μm).

To study changes in Fa2p-HA localization during flagellar regeneration, we deflagellated *fa2*-1; *FA2*-HA cells by pH shock and harvested cells at various stages of flagellar assembly. At 5 min postdeflagellation, a robust bb-Fa2p-HA signal is observed, along with faint staining of ax-Fa2p-HA (Figure 5C). As the flagella grow, the intensity of the ax-Fa2p-HA signal increases, whereas the bb-Fa2p-HA signal diminishes (Figure 5C). Finally, by 90 min when the flagella have attained full length, no bb-Fa2p signal is observed (Figure 5C). These observations suggest that newly synthesized Fa2p is targeted to basal bodies and is deposited at the severing site as soon as the flagella grow past the transition zone.

Fa2p-HA Localization during Mitosis

We have previously reported that *fa2* cells delay at the G_2/M transition of the cell cycle (Mahjoub *et al*., 2002). It was, therefore, of interest to determine Fa2p localization during mitosis. *fa2*-1; *FA2*-HA cells were synchronized for growth,

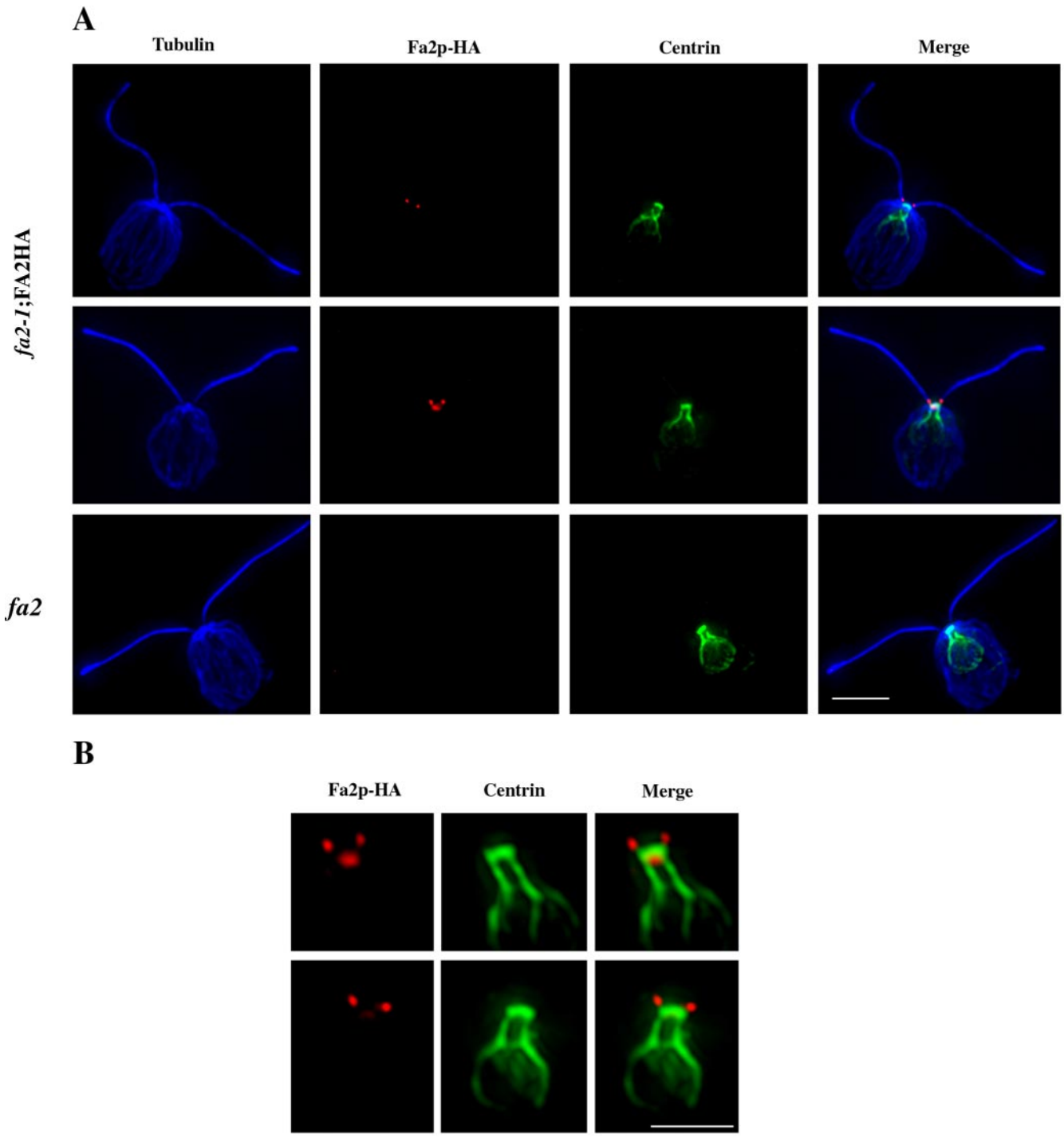

Figure 3. Fa2p localization in *Chlamydomonas* cells. (A) Triple-staining of *fa2*-1; *FA2*-HA cells (top two rows) and *fa2-1* mutant cells (bottom row) with anti-α-tubulin (blue), anti-HA (red), and anti-centrin (green) antibodies. Bar, 5 μm. (B) Magnification of the basal body-transition zone region showing two examples of Fa2p-HA and centrin costaining. Bar, 2 μm.

harvested during mitosis, and stained for Fa2p-HA. The cells also were stained for centrin and α-tubulin to identify the position of the basal bodies and microtubular structures, respectively. During prophase (an incipient cleavage furrow is visible at this stage; Kirk, 1998), the flagella have completely resorbed, the basal bodies have duplicated and are slightly separated at the anterior end of the cell (Figure 6, prophase). Note the colocalization of Fa2p-HA with each of the basal body spots. As cells progress through metaphase/anaphase, the basal bodies separate further and begin to serve as spindle pole microtubule organizing centers (Silflow and Lefebvre, 2001). In these cells, the Fa2p-HA signal is more diffuse and is associated with the proximal regions of the mitotic spindle (Figure 6, top, in metaphase/anaphase). As cells progress through nuclear division and cytokinesis, Fa2p-HA remains tightly associated with the

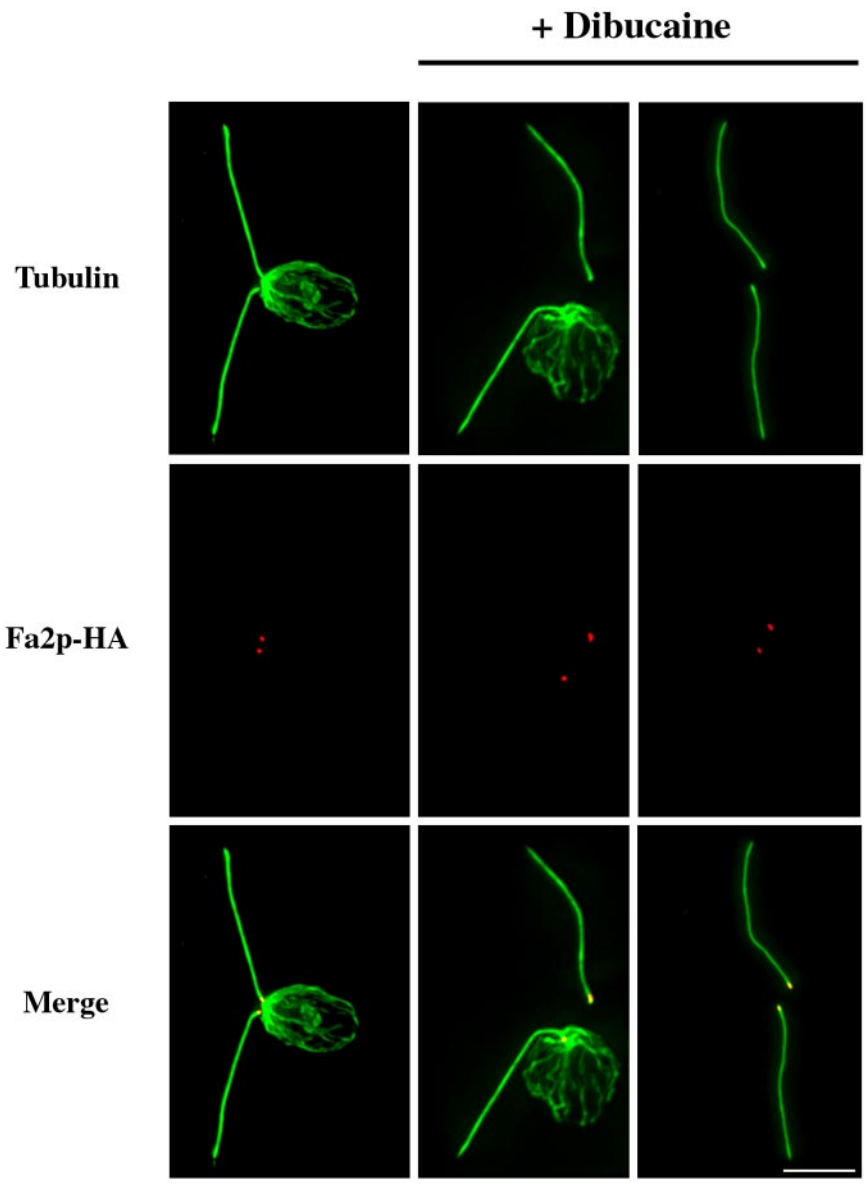

Figure 4. Axonemal Fa2p localizes distal to the site of axonemal microtubule severing. *fa2*-1; *FA2*-HA cells were spotted onto polyethylenimine-coated coverslips and briefly allowed to adhere. Cells were deflagellated by addition of dibucaine and immediately fixed with methanol. Samples were subsequently stained with anti-HA (red) and anti-α-tubulin (green) antibodies. Bar, 5 μm.

basal bodies in each newly formed daughter cell (Figure 6, cytokinesis). During the onset of G1 phase, daughter cells begin to assemble flagella. The ax-Fa2p-HA signals are apparent at this early stage of postmitotic flagellar assembly (Figure 6, G1 onset). Images from this stage are comparable with the signals observed in cells that are regenerating their flagella 5 min after deflagellation (Figure 5C).

Fa2p Kinase Activity Is Required for Deflagellation, but Not for Cell Cycle Progression

Although Fa2p is essential for calcium-induced deflagellation (Finst *et al*., 1998), and we have now shown that this kinase localizes to the site of axonemal severing (Figure 4), previous data suggested that kinase activity was not required for axonemal severing. Lohret *et al*. (1998) found that in vitro activation of axonemal severing by calcium did not require the addition of ATP and was not blocked by nonhydrolyzable ATP analogues or ADP. Based on these data, we hypothesized that the kinase activity of Fa2p plays a role in the assembly of a severing complex, rather than a signaling role during stress-induced deflagellation. To test this idea, we constructed a presumptive catalytically inactive (kinase-dead) version of the protein, by using site-directed mutagenesis to convert the invariant lysine in the ATP-binding loop to an arginine (Figure 7A, Fa2p-HA-K46R). The cognate mutation has been shown to inactivate kinase activity in several other Nek kinases (Noguchi *et al*., 2002; Faragher and Fry, 2003; Yin *et al*., 2003; Twomey *et al*., 2004). The construct was transformed into *fa2-1* mutant cells, and transformants were assayed for expression of the protein. Approximately 18% of transformants (n = 33) expressed a protein of the expected size (Figure 7A). Whereas *fa2* mutants expressing the Fa2p-HA were rescued for the deflagellation defect, none of the cells expressing the Fa2p-HA-K46R were rescued (Figure 7A). This result indicates that kinase activity is necessary for deflagellation.

To determine whether failure to rescue the deflagellation defect was due to mislocalization of the kinase-dead protein, we stained the cells with anti-HA antibodies. The Fa2p-HA-K46R localizes to the same region of the axoneme as

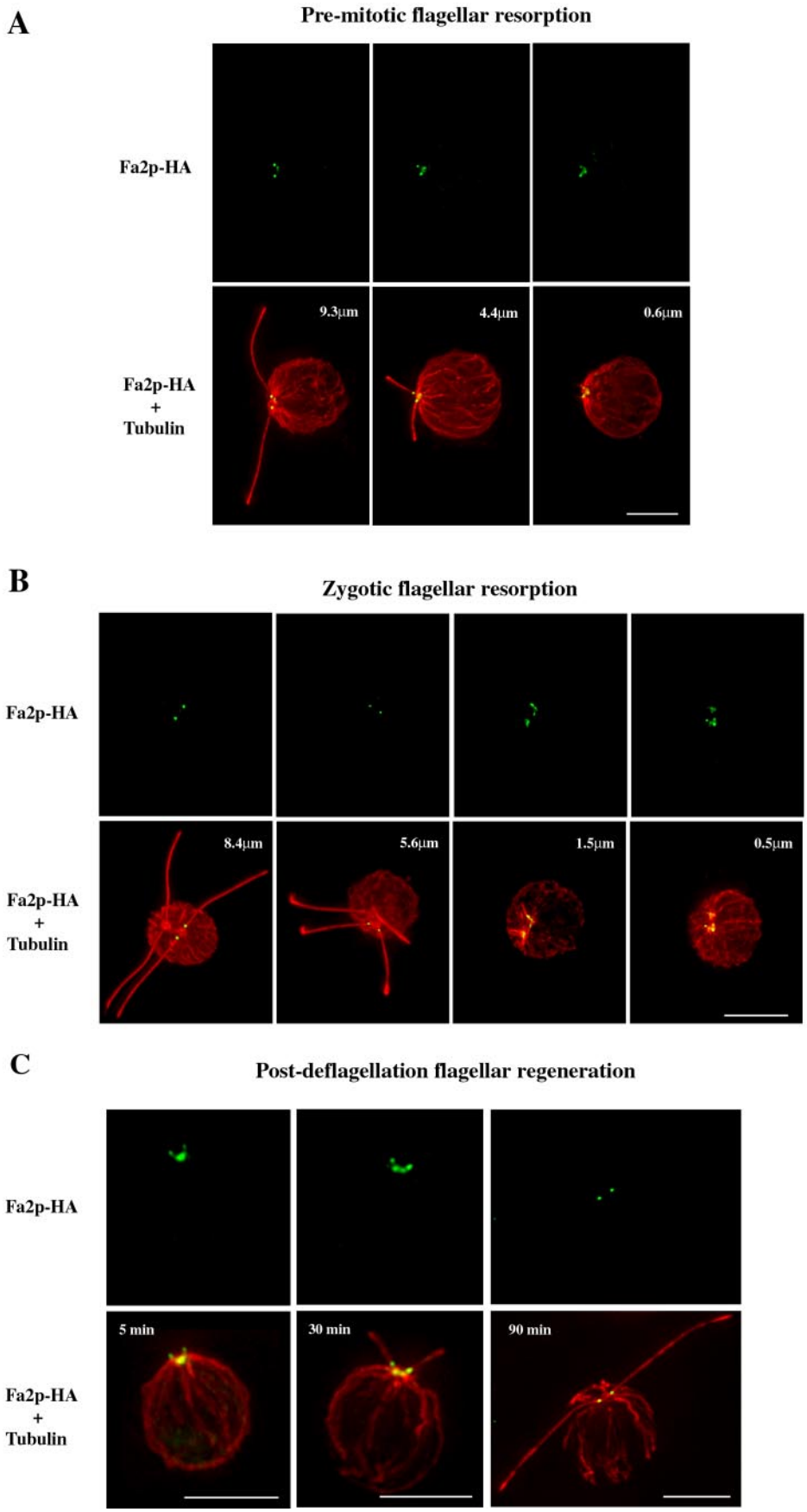

Figure 5. Dynamic changes in basal body-associated and axonemal Fa2p levels during flagellar resorption and assembly. (A) Cultures of *fa2*-1; *FA2*-HA cells were synchronized and harvested during a period of flagellar resorption, before entry into mitosis. Cells were stained with anti-HA (green) and anti-α-tubulin (red) antibodies. Both flagella from the represented cells were measured, and the average length indicated in the bottom panels. (B) *fa2*-1; *FA2*-HA and wild-type cells were transferred to medium lacking nitrogen and grown overnight to induce gametogenesis. The resulting gametes were mixed together to allow mating and formation of QFCs. To obtain cells at various stages of flagellar resorption, samples were collected at 30-min intervals for the next 4 h. Samples were fixed and stained with anti-HA (green) and anti-α-tubulin (red) antibodies. Both flagella from the original Fa2p-HA-expressing cell were measured, and the average length indicated in the bottom panels. (C) *fa2*-1; *FA2*-HA cells were deflagellated by pH shock and allowed to regenerate their flagella. Samples were taken at 5, 30 and 90 min post-deflagellation; fixed; and stained with antibodies for HA (green) and α-tubulin (red). Bars, 5 μm.

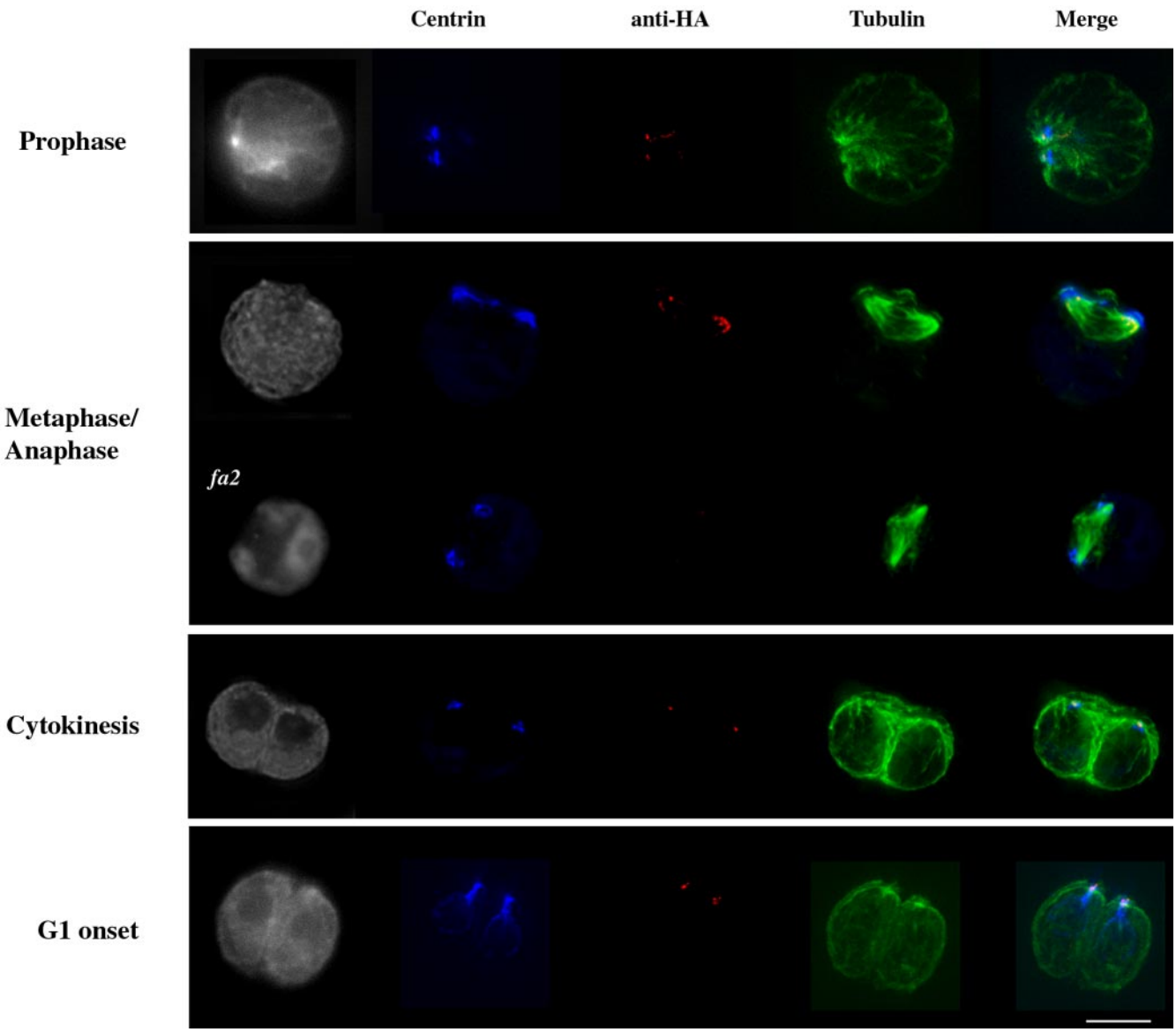

Figure 6. Fa2p localization during mitosis in *Chlamydomonas*. Synchronized *fa2*-1; *FA2*-HA cells were harvested as cells were beginning to divide. Samples were fixed and stained with antibodies for centrin (blue), HA (red), and α-tubulin (green). Also, cell autofluorescence is shown in the far-left column and helps identify the position of the nucleus. Representative samples of cells in prophase, metaphase/anaphase, cytokinesis, and the onset of G1 are shown. To determine the specificity of Fa2p-HA staining in dividing cells, *fa2* mutants were synchronized and stained as described above (our unpublished data, except for a metaphase/anaphase cell, the phase at which we saw the highest nonspecific staining).

Fa2p-HA (Figure 7B). This indicates that kinase activity of Fa2p is not required for its localization to the site of severing. The role of Fa2p kinase activity in the deflagellation pathway remains to be determined.

We next asked whether the cell cycle function of Fa2p requires its kinase activity. Our presumptive kinase-dead Fa2p-HA-K46R localized correctly to both the proximal axoneme and basal bodies (Figure 7B; our unpublished data) but did not fulfill the deflagellation function of wild-type Fa2p. This provided us with an opportunity to test whether the G_2/M delay of *fa2* mutants was a consequence of defects in axonemal severing, or due to some other function of the protein. We hypothesized that the cell cycle delay would be directly related to the deflagellation defect because flagella are resorbed at G_2/M and the mechanisms of resorption and deflagellation share common features (Parker and Quarmby, 2003). We initially used cell size as a proxy for cell cycle progression (Mahjoub *et al*., 2002). As shown in Figure 7C, Fa2p-HA-K46R rescues the cell size phenotype of *fa2* mutant cells. To directly assess whether the mutant protein had indeed rescued the cell cycle progression delay, we measured mitotic index. Figure 7D shows that *fa2*-1; *FA2*HA-K46R cells enter mitosis at the same time as wild-type cells, ~4 h sooner than *fa2*-1 cells. Although we did not predict this result, it is consistent with recent observations in *Xenopus* mitosis, where a vertebrate NIMA-related kinase, Nek2B, plays an important role in centrosome assembly (Fry *et al*., 1998). A confirmed kinase-dead mutant Nek2B localizes correctly to the centrosome and satisfies the centrosome duplication function of Nek2B (Twomey *et al*., 2004).

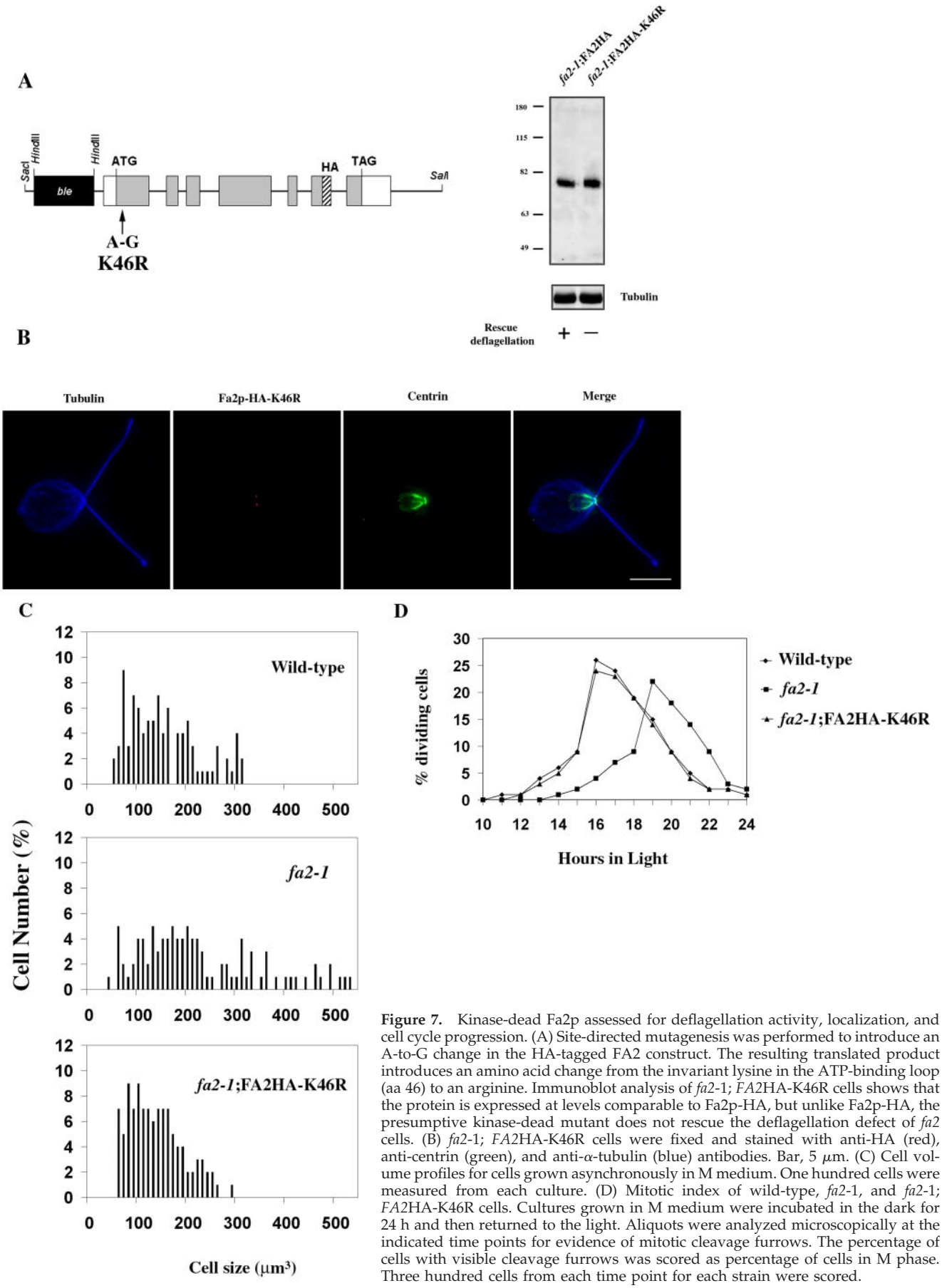

Figure 7. Kinase-dead Fa2p assessed for deflagellation activity, localization, and cell cycle progression. (A) Site-directed mutagenesis was performed to introduce an A-to-G change in the HA-tagged FA2 construct. The resulting translated product introduces an amino acid change from the invariant lysine in the ATP-binding loop (aa 46) to an arginine. Immunoblot analysis of *fa2*-1; *FA2*HA-K46R cells shows that the protein is expressed at levels comparable to Fa2p-HA, but unlike Fa2p-HA, the presumptive kinase-dead mutant does not rescue the deflagellation defect of *fa2* cells. (B) *fa2*-1; *FA2*HA-K46R cells were fixed and stained with anti-HA (red), anti-centrin (green), and anti-α-tubulin (blue) antibodies. Bar, 5 μm. (C) Cell volume profiles for cells grown asynchronously in M medium. One hundred cells were measured from each culture. (D) Mitotic index of wild-type, *fa2*-1, and *fa2*-1; *FA2*HA-K46R cells. Cultures grown in M medium were incubated in the dark for 24 h and then returned to the light. Aliquots were analyzed microscopically at the indicated time points for evidence of mitotic cleavage furrows. The percentage of cells with visible cleavage furrows was scored as percentage of cells in M phase. Three hundred cells from each time point for each strain were scored.

Fa2p Localization in Mouse Kidney Cells

Deflagellation (or deciliation) is a ubiquitous cellular response to stress (reviewed in Quarmby, 2004). We previously noted that expansion of the Nek family of proteins correlates with the presence of cilia (Bradley *et al*., 2004). Although we cannot identify a mammalian ortholog of Fa2p on the basis of sequence data, it falls in the same phylogenetic group as Nek 1/3/4/8 (Bradley *et al*., 2004). We anticipate that this group retains responsibility for the conduct of certain fundamental cellular functions, such as deflagellation and cell cycle progression. Consequently, we hypothesized that Fa2p would localize in mammalian cells as it does in *Chlamydomonas*, reflecting the localization of an as yet unidentified functional ortholog. To express Fa2p in mammalian cells, the *FA2* cDNA was cloned into a mammalian expression vector containing the gene encoding the enhanced green fluorescence protein (EGFP). The resulting product would be expressed as an EGFP-Fa2p chimera.

The EGFP-FA2 construct was transfected into mouse kidney collecting duct epithelial cells (IMCD-3). Immunoblots of whole cell lysate with anti-GFP antibodies showed a single band of the expected molecular weight in transfected cells (Figure 8A, left). This band is not detected in control cells transfected with EGFP-only. Immunoblots of the same cell lysates with the anti-Fa2p antibody recognized the same band (Figure 8A, right).

Fluorescence microscopy revealed an EGFP-Fa2p signal at the base of the primary cilium (Figure 8, B and C). Localization of Fa2p to the proximal end of the cilium is of particular interest because the simplest hypothesis is that it is axonemal Fa2p that is required for deflagellation in *Chlamydomonas*. Although it is not clear that deciliation is a part of the normal physiology of epithelial cells, many different cell types have been observed to deciliate in response to stress (reviewed in Quarmby, 2004). Independent of the physiological relevance of deciliation, ax-Fa2p (or its ortholog) may play a role in coordinating ciliary assembly/disassembly and cell cycle progression, for example, by sequestration of Fa2p (or associated proteins) in the cilia when cells are in interphase.

There is also a distinct EGFP-Fa2p signal associated with the proximal end of the centrioles in the kidney cells (Figure 8, B and C). Note that in mammalian cells the centrioles are orthogonally positioned, so that the proximal regions of each centriole are distant from one another. This is in contrast to the closely apposed proximal regions of the *Chlamydomonas* basal bodies (Figure 3; reviewed in Kirk, 1998). The centriolar staining pattern observed in Figure 8 supports our suggestion that bb-Fa2p is associated with the proximal basal bodies. In transfected IMCD-3 cells undergoing division, EGFP-Fa2p remained associated with centrioles throughout mitosis (Figure 9). As in *Chlamydomonas*, Fa2p signals were observed associated with the base of each new daughter centriole (Figure 9, top). As cells progressed into metaphase, there was robust EGFP-Fa2p staining at the spindle poles (Figure 9, middle). Finally, as cells approached cytokinesis, EGFP-Fa2p was tightly associated with the centrioles in the new daughter cells (Figure 9, bottom). Intriguingly, a significant EGFP-Fa2p signal was associated with acetylated microtubules at the midbody (Figure 9, arrow).

DISCUSSION

The proximal axoneme has received little attention as a specialized functional zone, but there are indications that this is about to change. Recent studies of the role of primary cilia as flow sensors (McGrath *et al*., 2003; Nauli *et al*., 2003; Praetorius *et al*., 2003) suggest that this region of the flagella is likely to play a role in mechanical sensation. It also may be an important site for the regulation of intraflagellar transport (IFT). IFT is the process by which cilia and flagella are built and maintained; it involves anterograde and retrograde transport of flagellar components along the axoneme (reviewed by Rosenbaum and Witman, 2002). When retrograde IFT is blocked, IFT particles and proteins accumulate at the proximal flagellum (Pazour *et al*., 1999; Porter *et al*., 1999; Iomini *et al*., 2004). Similarly, IFT proteins accumulate at this site in differentiated *Chlamydomonas* gametes, presumably in anticipation of a rapid burst of anterograde IFT upon mating (Lucker, Goodenough, and Cole, personal communication; Mesland *et al*., 1980; Musgrave and van den Ende, 1987). The idea that this site plays an important role in IFT is further supported by observations that many flagellar assembly, or *fla*, mutants have deflagellation phenotypes and the *fa1* and *fa2* deflagellation-defective mutants have flagellar resorption phenotypes (Parker and Quarmby, 2003; Parker and Quarmby, unpublished data). In the present report, we show that an NIMA-family kinase, Fa2p, localizes to the proximal end of the axoneme in both *Chlamydomonas* and mouse kidney cells (Figures 2–4 and 8). In this context, it is interesting to note that KIF3A (the anterograde kinesin of IFT) has recently been identified as a putative substrate of human Nek1 (Surpili *et al*., 2003). We propose that this specialized region of the proximal cilium be known as the site of flagellar assembly/autotomy (SOFA). Fa2p lies on the SOFA.

Axonemal Fa2p localizes to the distal side of the site where the outer doublet microtubules are severed during stress-induced deflagellation (Figure 4; Lewin and Lee, 1985). This location is perhaps not surprising, given that *fa2* cells are defective in one of the final steps of deflagellation: calcium-activated microtubule severing (Finst *et al*., 1998). However, the role of a kinase in this pathway is perplexing because earlier results indicated that ATP is not required for calcium-activated axonemal severing. We previously developed an in vitro assay for axonemal microtubule severing wherein axonemal-basal body complexes are isolated from whole cells in the presence of calcium chelators (Lohret *et al*., 1998). Calcium, but not ATP, is necessary to activate axonemal severing in this system, and axonemal-basal body complexes from *fa2* cells do not sever in response to calcium addition (Lohret *et al*., 1998). These data suggest that the Fa2p kinase was not likely to play a direct role in signaling calcium-induced deflagellation, but they may be important for directing assembly of a microtubule severing complex during axonemal assembly (Mahjoub *et al*., 2002). Therefore, localization of Fa2p near the site of severing suggested that either its role in severing was kinase-independent, or its kinase activity was required for the priming or assembly of additional factors at this site. Correct localization of a kinase-dead Fa2p to the proximal axoneme, without rescue of the deflagellation-defect of *fa2* cells (Figure 7) clearly demonstrates that its role in deflagellation is not kinase independent. We conclude that Fa2p itself targets to this site in a kinase-independent manner, but that its kinase activity is important for the assembly of a severing complex.

To our surprise, the kinase-dead Fa2p rescued the cell cycle progression delay of *fa2* mutant cells (Figure 7). Because *fa2;fla10-1* double mutants are slow to resorb their flagella on shift to the restrictive temperature (Parker and Quarmby, 2003), we thought that the G_2/M delay of *fa2* mutants might be a consequence of slow flagellar resorption before M phase. However, another mutant with defective

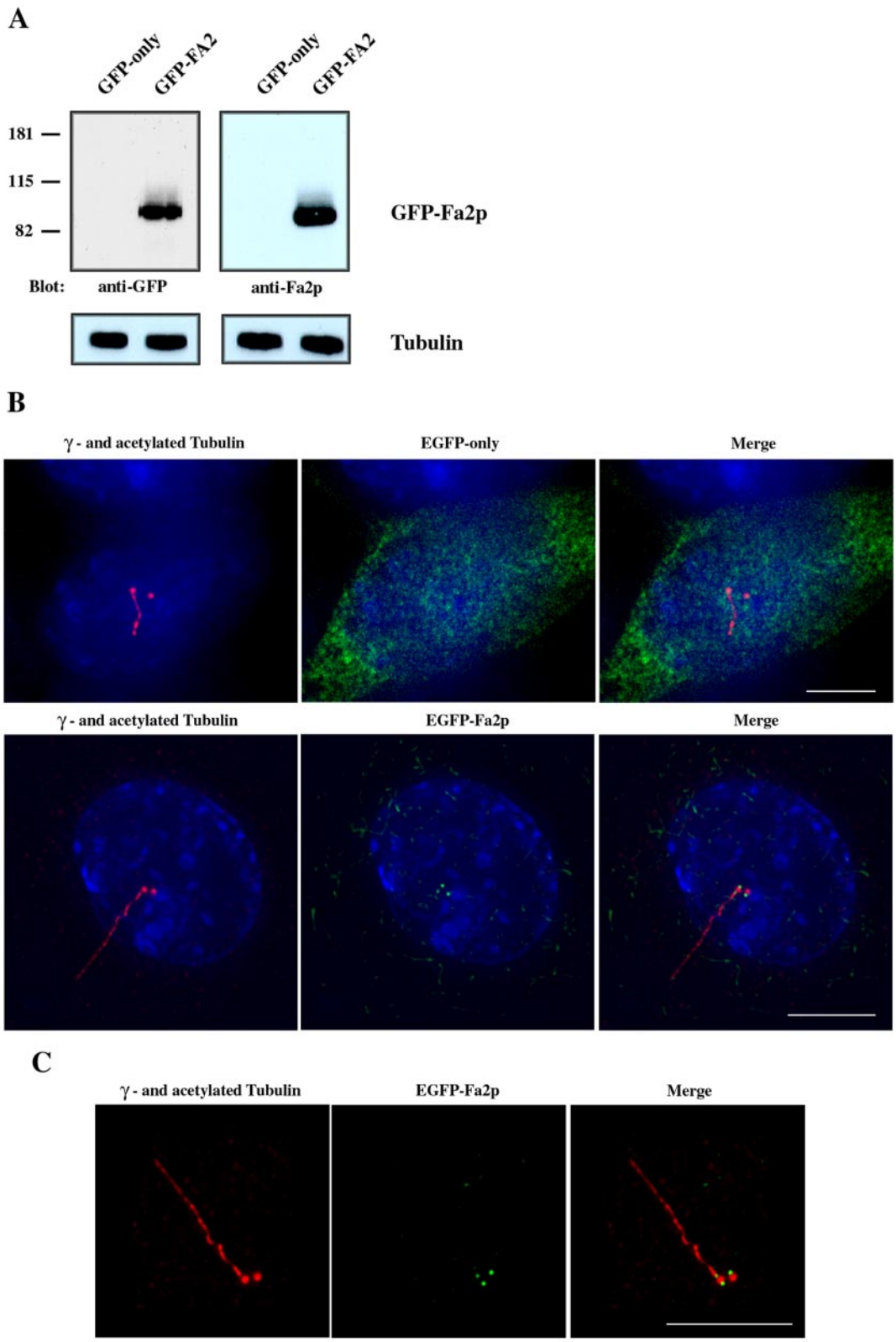

Figure 8. Expression of Fa2p in mouse kidney cells. (A) IMCD-3 cells were transfected with an expression vector containing either EGFP-FA2 or EGFP only as a control. Immunoblots of total protein extract were probed with anti-GFP and anti-Fa2p antibodies. The membranes were stripped and reprobed with anti-α-tubulin antibody for loading control. Molecular mass standards (in kilodlatons) are indicated on the left. (B) Cells transfected with EGFP-only (top) or EGFP-FA2 (bottom) were costained with antibodies against γ- and acetylated tubulin, to mark the positions of the centrioles and the cilia, respectively. A common secondary antibody was used that allowed visualization of both γ- and acetylated tubulin (red), and EGFP-Fa2p was visualized directly using the fluorescein channel (green). DNA was stained with DAPI (blue). (C) Magnified image from EGFP-Fa2p expressing cell in B showing relative position of the centrioles, cilium, and Fa2p. The image was rendered 140° around the *x*-axis and magnified 1.5×. Bars, 5 μm.

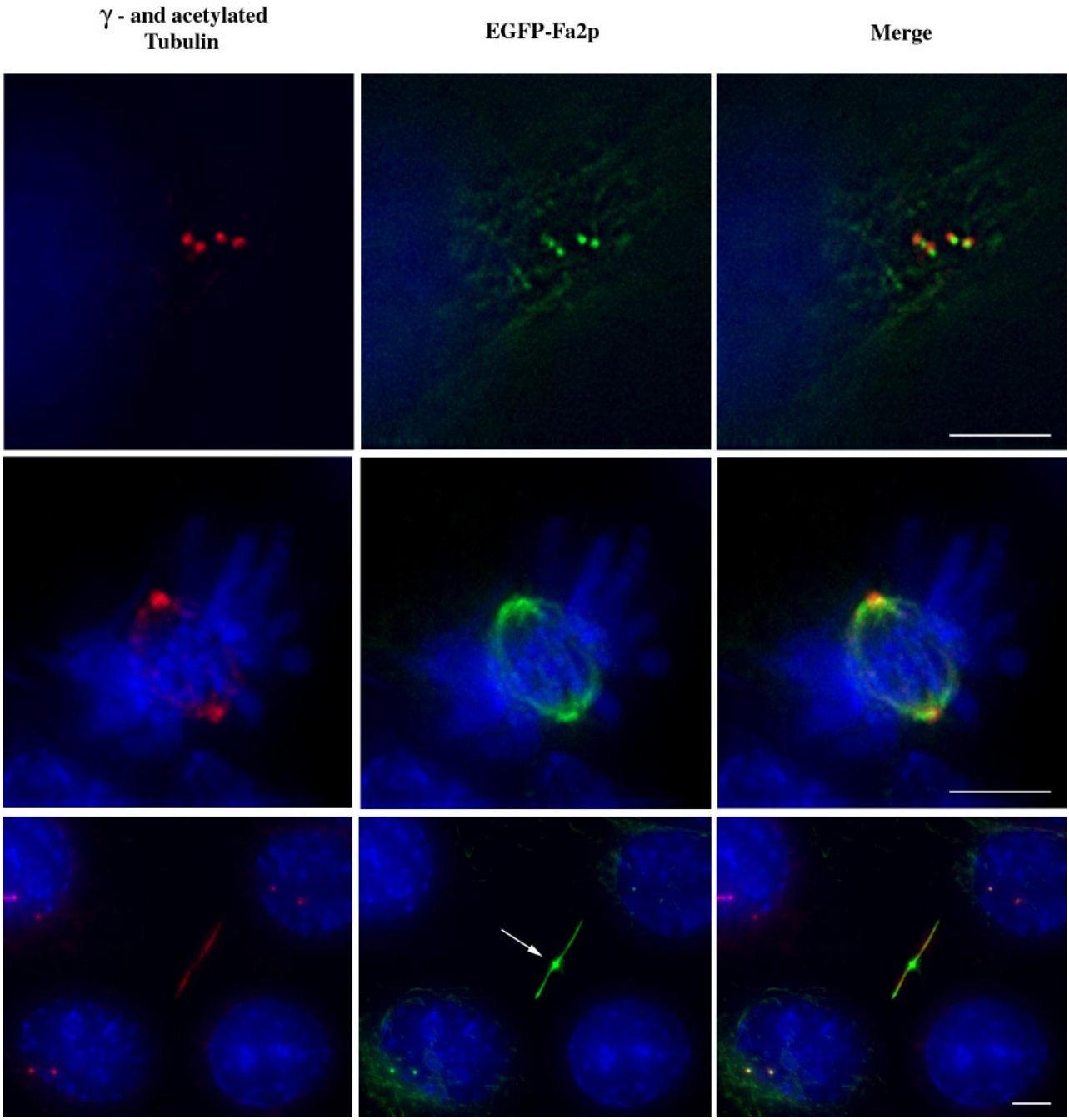

Figure 9. Fa2 localization during mitosis in mouse kidney cells. IMCD-3 cells expressing EGFP-Fa2p were stained for γ- and acetylated tubulin (red), and cells were visualized at various stages of division. Images shown are from cells after centriole duplication (top), metaphase (middle), and cytokinesis (bottom). Arrow indicates concentration of EGFP-Fa2p signal in the middle of the cytoplasmic microtubule bridge connecting the dividing cells. Bars, 5 μm.

calcium-activated axonemal severing, *fa1*, does not have a G_2/M delay (our unpublished data), yet it is also slow to resorb flagella as a *fa1;fla10-1* double mutant at the restrictive temperature (Parker and Quarmby, 2003). Together, these data support the idea that the cell cycle progression phenotype of *fa2* cells is independent of its kinase-dependent axonemal severing function. Consistent with this is a recent report that Nek2B has a kinase-independent role in centrosome assembly (Twomey *et al*., 2004).

In *Chlamydomonas* and in kidney cells, Fa2p localized to the proximal end of basal bodies and centrioles respectively (Figures 3–6, 8, and 9). It was observed at the base of daughter as well as mother basal bodies and centrioles, but it is not required for basal body assembly, nor for the assembly of flagella (Finst *et al*., 1998). In both cell types, Fa2p remained associated with the spindle poles throughout mitosis (Figures 6 and 9). In *Chlamydomonas*, Fa2p occurred at the proximal cilium at the onset of G_1 (we did not capture

any IMCD-3 cells at this precise stage of cell division). In the IMCD-3 cells, we noticed an additional site of localization of Fa2p during cell division: the midbody or cytoplasmic bridge between two cells at the final stages of cytokinesis. Acetylated microtubules span the midbody (Figure 9; our unpublished data) and an intense Fa2p signal is observed approximately midway along the length of these microtubules (Figure 9). The staining that we observed in this region looks very much like the staining of midbody complex proteins, the mitotic kinesin-like protein CHO1 (Matuliene and Kuriyama, 2002), and the calcium-binding protein Annexin 11 (Tomas *et al*., 2004). The axonemal microtubules whose calcium-induced severing is Fa2p dependent also are acetylated, and we speculate that an ortholog of Fa2p may play a role in the severing of acetylated microtubules during the final stages of cytokinesis in the kidney cells. Fa2p is not predicted to play a similar role in the cytokinesis of *Chlamydomonas* because an analogous structure does not form (Johnson and Porter, 1968; Ehler and Dutcher, 1998).

Mice with mutations in either Nek1 or Nek8 have pleiotropic phenotypes, including cystic kidneys (Upadhya *et al*., 2000; Liu *et al*., 2002). Our discovery that a member of this phylogenetic group of Nek proteins, Fa2p, is localized to the same subcellular sites in both *Chlamydomonas* and kidney epithelial cells provides strong support for the concept that this family of kinases plays conserved roles in the coordination of cilia and cell cycle progression. This conservation is important because it will allow the application of the powerful genetic, molecular, and biochemical approaches available in *Chlamydomonas* to critical questions, such as the identification of the key substrates and interacting proteins in this human disease-related pathway.

ACKNOWLEDGMENTS

We are grateful to many members of the research community for stimulating discussions. We are particularly indebted to the following colleagues: Jeff Salisbury and Saul Purton generously provided the centrin antibody and pSP124S vector, respectively. B.J. Lucker, Ursula Goodenough, and Doug Cole kindly shared their unpublished observations and ruminations on IFT proteins at the proximal flagella of gametes. Wallace Marshall suggested the QFC experiment, and Ben Goh helped generate the kinase-dead *FA2* construct. Michel Leroux and Jun Chul Kim enabled the kidney cell experiments. M.R.M. was supported, in part, by Doctoral Fellowships from the Michael Smith Foundation for Health Research, and the Natural Sciences and Engineering Research Counsel. This work was supported by an operating grant to L.M.Q. from the Canadian Institutes of Health Research (MOP 37861).

REFERENCES

Berman, S.A., Wilson, N.F., Haas, N.A., and Lefebvre, P.A. (2003). A novel MAP kinase regulates flagellar length in *Chlamydomonas*. Curr. Biol. *13*, 1145–1149.

Bradley, B.A., Wagner, J.J.D., and Quarmby, L.M. (2004). Identification and sequence analysis of six new members of the NIMA-related kinase family in *Chlamydomonas*. J. Eukaryot. Microbiol. *51*, 66–72.

Cavalier-Smith, T. (1974). Basal body and flagellar development during the vegetative cell cycle and the sexual cycle of *Chlamydomonas reinhardtii*. J. Cell Sci. *16*, 529–556.

Dutcher, S.K., Morrissette, N.S., Preble, A.M., Rackley, C., and Stanga, J. (2002). Epsilon-tubulin is an essential component of the centriole. Mol. Biol. Cell *13*, 3859–3869.

Ehler, L.L., Holmes, J.A., and Dutcher, S.K. (1995). Loss of spatial control of the mitotic spindle apparatus in a *Chlamydomonas reinhardtti* mutant strain lacking basal bodies. Genetics *141*, 945–960.

Ehler, L.L., and Dutcher, S.K. (1998). Pharmacological and genetic evidence for a role of rootlet and phycoplast microtubules in the positioning and assembly of cleavage furrows in *Chlamydomonas reinhardtii*. Cell Motil. Cytoskeleton *40*, 193–207.

Faragher, A.J., and Fry, A.M. (2003). Nek2A kinase stimulates centrosome disjunction and is required for formation of bipolar mitotic spindles. Mol. Biol. Cell *14*, 2876–2889.

Finst, R.J., Kim, P.J., and Quarmby, L.M. (1998). Genetics of the deflagellation pathway of *Chlamydomonas reinhardtii*. Genetics *149*, 927–936.

Finst, R.J., Kim, P.J., Griffis, E., and Quarmby, L.M. (2000). Fa1p is a 171 kDa protein essential for axonemal microtubule severing in *Chlamydomonas*. J. Cell Sci. *113*, 1963–1971.

Fry, A.M., Meraldi, P., and Nigg, E.A. (1998). A centrosomal function for the human Nek2 protein kinase, a member of the NIMA family of cell cycle regulators. EMBO J. *17*, 470–481.

Harris, E.H. (1989). The Chlamydomonas Sourcebook, Berkeley, CA: Academic Press.

Huangfu, D., Liu, A., Rakeman, A.S., Murcia, N.S., Niswander, L., and Anderson, K.V. (2003). Hedgehog signalling in the mouse requires intraflagellar transport proteins. Nature *426*, 83–87.

Iomini, C., Tejada, K., Mo, W., Vaananen, H., and Piperno, G. (2004). Primary cilia of human endothelial cells disassemble under laminar shear stress. J. Cell Biol. *164*, 811–817.

Johnson, U.G., and Porter, K.R. (1968). Fine structure of cell division in *Chlamydomonas reinhardi*. Basal bodies and microtubules. J. Cell Biol. *38*, 403–425.

Kambouris, N.G., Burke, D.J., and Creutz, C.E. (1993). Cloning and genetic analysis of the gene encoding a new protein kinase in *Saccharomyces cerevisiae*. Yeast *9*, 141–150.

Kirk, D.L. (1998). Volvox. In: Molecular-Genetic Origins of Multicellularity and Cellular Differentiation, New York, NY: Cambridge University Press.

Krien, M.J., Bugg, S.J., Palatsides, M., Asouline, G., Morimyo, M., and O'Connell, M.J. (1998). A NIMA homologue promotes chromatin condensation in fission yeast. J. Cell Sci. *111*, 967–976.

Lewin, R.A., and Lee, K.W. (1985). Autotomy of algal flagella: electron microscope studies of *Chlamydomonas* (Chlorophyceae) and *Tetraselmis* (Prasinophyceae). Phycologia *24*, 311–316.

Li, J.B., *et al*. (2004). Comparative genomics identifies a flagellar and basal body proteome that includes the BBS5 human disease gene. Cell *117*, 541–552.

Liu, S., Lu, W., Obara, T., Kuida, S., Lehoczky, J., Dewar, K., Drummond, I.A., and Beier, D.R. (2002). A defect in a novel Nek-family kinase causes cystic kidney disease in the mouse and in zebrafish. Development *129*, 5839–5846.

Lohret, T.A., McNally, F.J., and Quarmby, L.M. (1998). A role for katanin-mediated axonemal microtubule severing in *Chlamydomonas* deflagellation. Mol. Biol. Cell *9*, 1195–1207.

Lumbreras, V., *et al*. (1998). Efficient foreign gene expression in *Chlamydomonas reinhardtii* mediated by an endogenous intron. Plant J. *14*, 441–448.

Mahjoub, M., Montpetit, B., Zhao, L., Finst, R.J., Goh, B., Kim, A.C., and Quarmby, L.M. (2002). The *FA2* gene of *Chlamydomonas* encodes a NIMA family kinase with roles in cell cycle progression and microtubule severing during deflagellation. J. Cell Sci. *115*, 1759–1768.

Matuliene, J., and Kuriyama, R. (2002). Kinesin-like protein CHO1 is required for the formation of midbody matrix and the completion of cytokinesis in mammalian cells. Mol. Biol. Cell *13*, 1832–1845.

McGrath, J., Somlo, S., Makova, S., Tian, X., and Brueckner, M. (2003). Two populations of node monocilia initiate left-right asymmetry in the mouse. Cell *114*, 61–73.

Mesland, D.A., Hoffman, J.L., Caligor, E., and Goodenough, U.W. (1980). Flagellar tip activation stimulated by membrane adhesions in *Chlamydomonas* gametes. J. Cell Biol. *84*, 599–617.

Morris, N.R., and Enos, A.P. (1992). Mitotic gold in a mold: *Aspergillus* genetics and the biology of mitosis. Trends Genet. *8*, 32–37.

Musgrave, A., and van den Ende, H. (1987). How *Chlamydomonas* court their partners. Trends Biochem. Sci. *12*, 470–473.

Mykytyn, K., and Sheffield, V.C. (2004). Establishing a connection between cilia and Bardet-Biedl Syndrome. Trends Mol. Med. *10*, 106–109.

Nauli, S.M., *et al*. (2003). Polycystins 1 and 2 mediate mechanosensation in the primary cilium of kidney cells. Nat. Genet. *33*, 129–137.

Noguchi, K., Fukazawa, H., Murakami, Y., and Uehara, Y. (2002). Nek11, a new member of the NIMA family of kinases, involved in DNA replication and genotoxic stress responses. J. Biol. Chem. *277*, 39655–39665.

O'Connell, M.J., Krien, M.J.E., and Hunter, T. (2003). Never say never. The NIMA-related protein kinases in mitotic control. Trends Cell Biol. *13*, 221–228.

Ong, A.C., and Wheatley, D.N. (2003). Polycystic kidney disease–the ciliary connection. Lancet *361*, 774–776.

Pan, J., Wang, Q., and Snell, W.J. (2004). An aurora kinase is essential for flagellar disassembly in *Chlamydomonas*. Dev. Cell *6*, 445–451.

Parker, J.D.K., and Quarmby, L.M. (2003). *Chlamydomonas fla* mutants reveal a link between deflagellation and intraflagellar transport. BMC Cell Biol. *4*, 11.

Pazour, G.J., Dickert, B.L., and Witman, G.B. (1999). The DHC1b (DHC2) isoform of cytoplasmic dynein is required for flagellar assembly. J. Cell Biol. *144*, 473–481.

Pazour, G.J., and Witman, G.B. (2003). The vertebrate primary cilium is a sensory organelle. Curr. Opin. Cell Biol. *15*, 105–110.

Pedersen, L.B., Geimer, S., Sloboda, R.D., and Rosenbaum, J.L. (2003). The microtubule plus end-tracking protein EB1 is localized to the flagellar tip and basal bodies in *Chlamydomonas reinhardtii*. Curr. Biol. *13*, 1969–1974.

Porter, M.E., Bower, R., Knott, J.A., Byrd, P., and Dentler, W. (1999). Cytoplasmic dynein heavy chain 1b is required for flagellar assembly in *Chlamydomonas*. Mol. Biol. Cell *10*, 693–712.

Praetorius, H.A., Frokiaer, J., Nielsen, S., and Spring, K.R. (2003). Bending the primary cilium opens Ca2+-sensitive intermediate-conductance K^+ channels in MDCK cells. J. Membr. Biol. *191*, 193–200.

Pu, R.T., Xu, G., Wu, L., Vierula, J., O'Donnell, K., Ye, X.S., and Osmani, S.A. (1995). Isolation of a functional homolog of the cell cycle-specific protein kinase NIMA of *Aspergillus nidulans* and functional analysis of conserved residues. J. Biol. Chem. *270*, 18110–18116.

Quarmby, L.M. (2004) Mechanism of cellular deflagellation. Int. Rev. Cytol. *233*, 47–91.

Rosenbaum, J.L., and Witman, G.B. (2002). Intraflagellar transport. Nat. Rev. Mol. Cell. Biol. *3*, 813–825.

Saito, T., and Matsuda, Y. (1991). Isolation and characterization of *Chlamydomonas* temperature-sensitive mutants affecting gametic differentiation under nitrogen-starved conditions. Curr. Genet. *19*, 65–71.

Salisbury, J.L., Baron, A.T., and Sanders, M.A. (1988). The centrin-based cytoskeleton of *Chlamydomonas reinhardtii*: distribution in interphase and mitotic cells. J. Cell Biol. *107*, 635–641.

Sanders, M.A., and Salisbury, J.L. (1989). Centrin-mediated microtubule severing during flagellar excision in *Chlamydomonas reinhardtii*. J. Cell Biol. *108*, 1751–1760.

Schneider, L., Hoffman, E.K., Satir, P., and Christensen, S.T. (2003). A mechanism for growth arrest control in the primary cilium based on PDGR-alpha. Mol. Biol. Cell *14*, 323a.

Silflow, C.D., and Lefebvre, P.A. (2001). Assembly and motility of eukaryotic cilia and flagella. Lessons from *Chlamydomonas reinhardtii*. Plant Physiol. *127*, 1500–1507.

Sun, Z., Amsterdam, A., Pazour, G.J., Cole, D.G., Miller, M.S., and Hopkins, N. (2004). A genetic screen in zebrafish identifies cilia genes as a principal cause of cystic kidney. Development *131*, 4085–4093.

Surpili, M.J., Delben, T.M., and Kobarg, J. (2003). Identification of proteins that interact with the central coiled-coil region of the human protein kinase NEK1. Biochemistry *42*, 15369–15376.

Tomas, A., Futter, C., and Moss, S.E. (2004). Annexin 11 is required for midbody formation and completion of the terminal phase of cytokinesis. J. Cell Biol. *165*, 813–822.

Tucker, R.W., and Pardee, A.B. (1979). Centriole ciliation is related to quiescence and DNA synthesis in 3T3 cells. Cell *17*, 527–535.

Twomey, C., S.L. Wattam, M.R., Rapley, J., Baxter, J.E., and Fry, A.M. (2004). Nek2B stimulates zygotic centrosome assembly in *Xenopus laevis* in a kinase-independent manner. Dev. Biol. *265*, 384–398.

Umen, J.G., and Goodenough, U.W. (2001). Control of cell division by a retinoblastoma protein homolog in *Chlamydomonas*. Genes Dev. *15*, 1652–1661.

Upadhya, P., Birkenmeier, E.H., Birkenmeier, C.S., and Barker, J.E. (2000). Mutations in a NIMA-related kinase gene, Nek1, cause pleiotropic effects including a progressive polycystic kidney disease in mice. Proc. Natl. Acad. Sci. USA *97*, 217–221.

Wang, D., Harper, J.F., and Gribskov, M. (2003). Systematic trans-genomic comparison of protein kinases between *Arabidopsis* and *Saccharomyces cerevisiae*. Plant Physiol. *132*, 2152–2165.

Wheatley, D.N., Wang, A.M., and Strugnell, G.E. (1996). Expression of primary cilia in mammalian cells. Cell Biol. Int. *20*, 73–81.

Wilson, P.D. (2004). Polycystic kidney disease. N. Engl. J. Med. *350*, 151–164.

Witman, G.B. (1986). Isolation of *Chlamydomonas* flagella and flagellar axonemes. Methods Enzymol. *134*, 280–290.

Yin, M.J., Shao, L., Voehringer, D., Smeal, T., and Jallal, B. (2003). The serine/threonine kinase Nek6 is required for cell cycle progression through mitosis. J. Biol. Chem. *278*, 52454–52460.